Cancer Cell, Volume *31*

Supplemental Information

Single-chromosome Gains Commonly Function as Tumor Suppressors

Jason M. Sheltzer, Julie H. Ko, John M. Replogle, Nicole C. Habibe Burgos, Erica S. Chung, Colleen M. Meehl, Nicole M. Sayles, Verena Passerini, Zuzana Storchova, and Angelika Amon

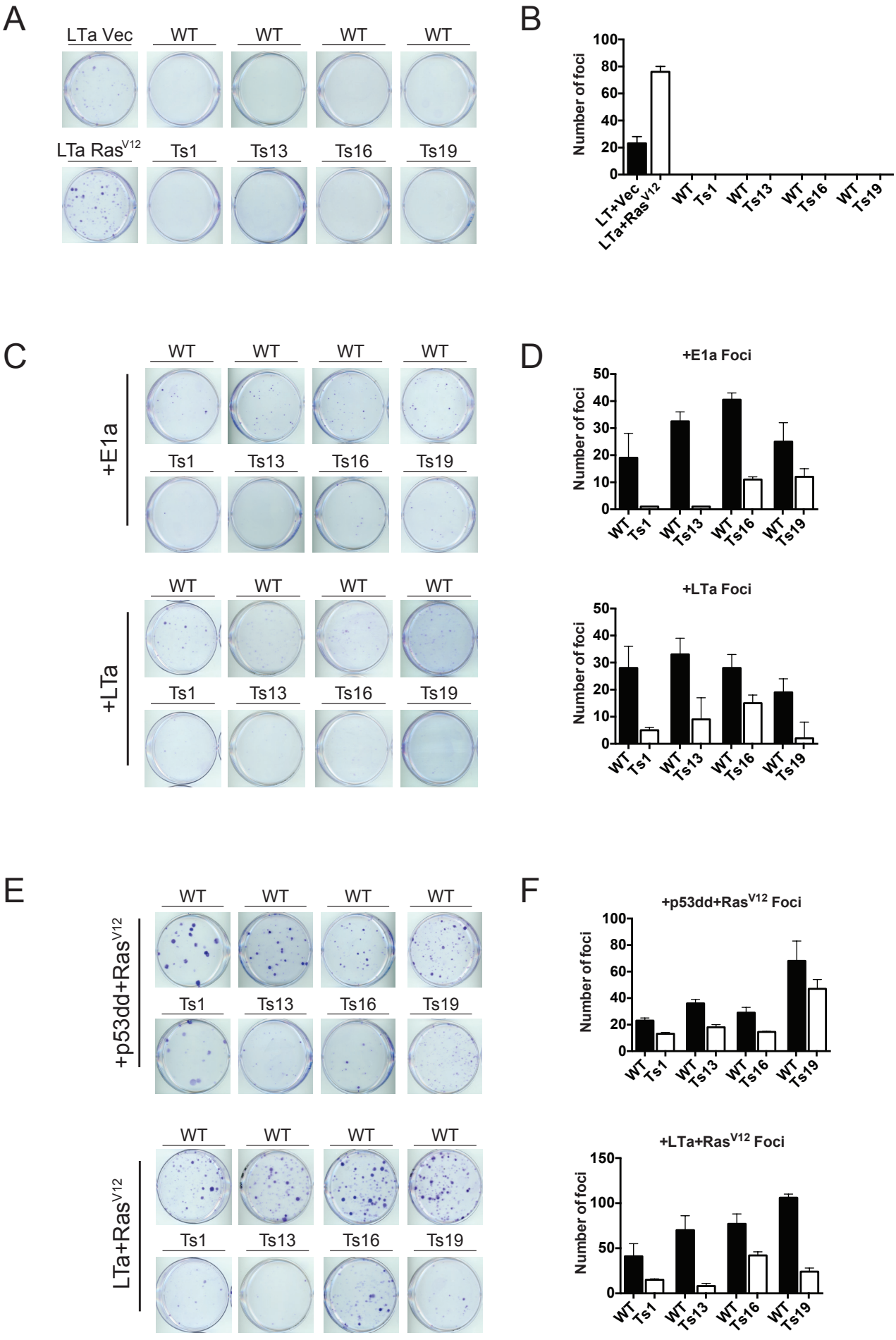
A
LTa Vec
WT
WT
WT
WT
LTa Ras^{V12}
Ts1
Ts13
Ts16
Ts19
B
Number of foci
100
80
60
40
20
0
LT+Vec
LTa+Ras^{V12}
WT
Ts1
WT
Ts13
WT
Ts16
WT
Ts19
C
+E1a
+LTa
WT
Ts1
Ts13
Ts16
Ts19
D
+E1a Foci
+LTa Foci
Number of foci
50
40
30
20
10
0
WT
Ts1
Ts13
Ts16
Ts19
E
+p53dd+Ras^{V12}
LTa+Ras^{V12}
F
+p53dd+Ras^{V12} Foci
+LTa+Ras^{V12} Foci
150
100
50

Figure S1, related to Figure 1. Trisomic fibroblasts display limited clonogenicity

(A) 1000 cells of the indicated cell lines were plated and grown for 10 days prior to staining with crystal violet. LTa-transduced MEFs are capable of forming colonies from single cells, but primary euploid and trisomic MEFs are non-clonogenic.

(B) Quantification of (A).

(C) Representative plates from a colony-formation assay of E1a or LTa-transduced MEFs.

(D) Quantification of (C).

(E) Representative plates from a colony-formation assay of Ras^{V12}-transduced MEFs.

(F) Quantification of (E). Error bars indicate the standard error of the mean.

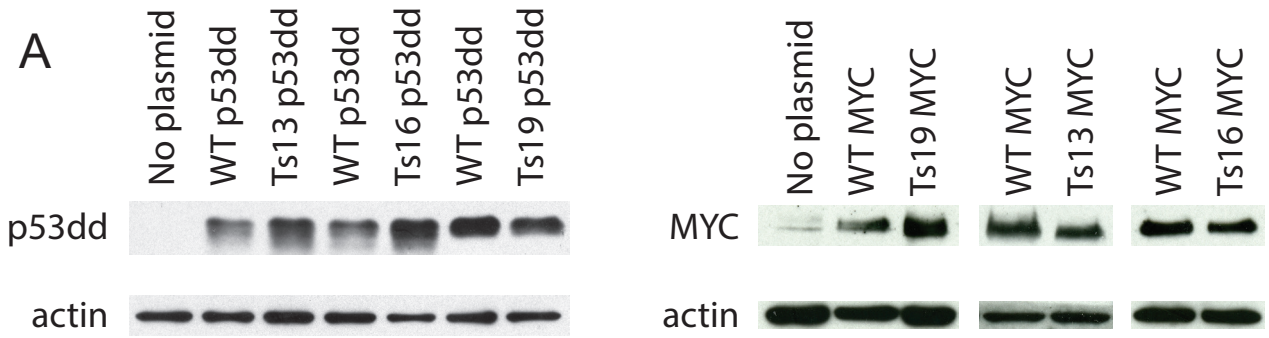
A
No plasmid
WT p53dd
Ts13 p53dd
WT p53dd
Ts16 p53dd
WT p53dd
Ts19 p53dd
p53dd
actin
No plasmid
WT MYC
Ts19 MYC
WT MYC
Ts13 MYC
WT MYC
Ts16 MYC
MYC
actin

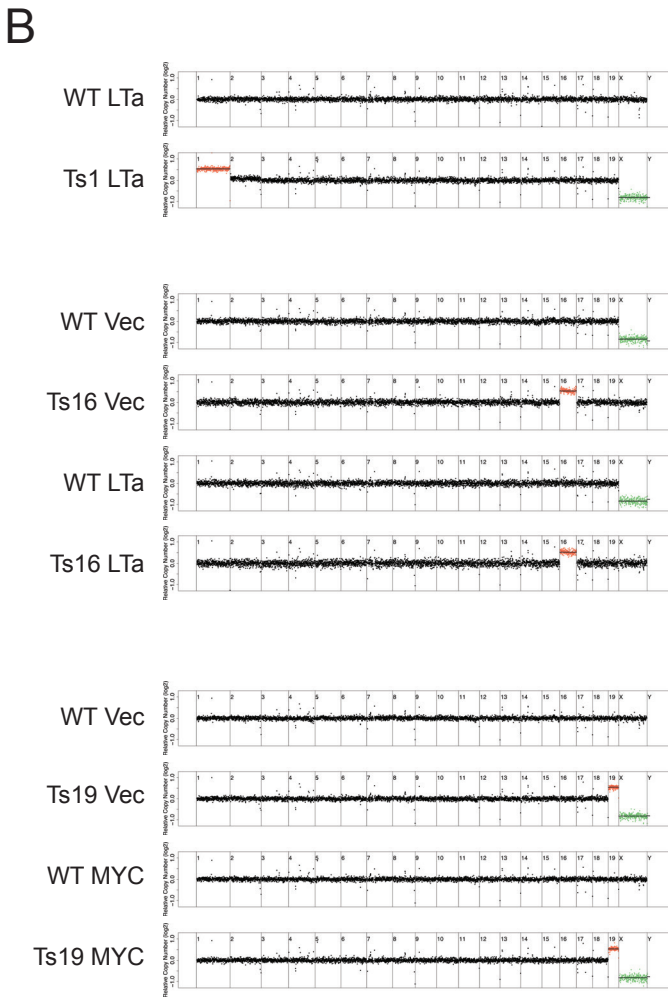
B
WT LTa
Ts1 LTa
WT Vec
Ts16 Vec
WT LTa
Ts16 LTa
WT Vec
Ts19 Vec
WT MYC
Ts19 MYC

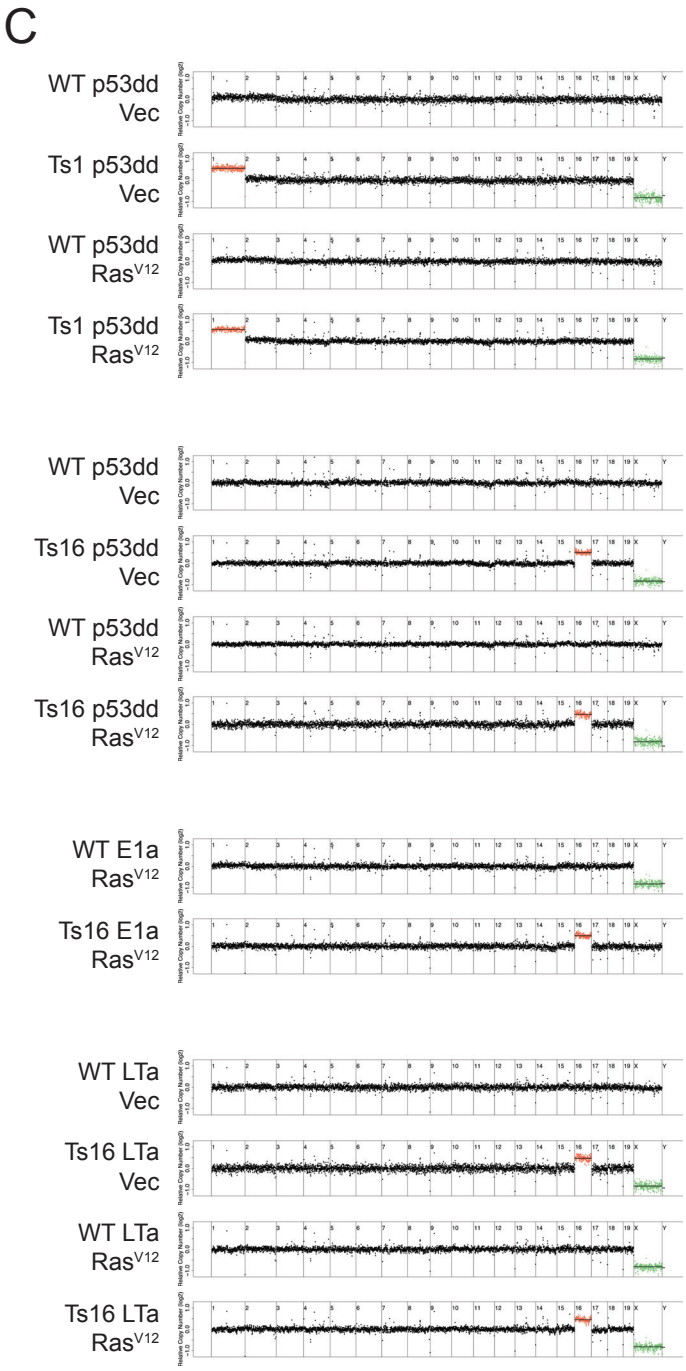
C
WT p53dd Vec
Ts1 p53dd Vec
WT p53dd RasV12
Ts1 p53dd RasV12
WT p53dd Vec
Ts16 p53dd Vec
WT p53dd RasV12
Ts16 p53dd RasV12
WT E1a RasV12
Ts16 E1a RasV12
WT LTa Vec
Ts16 LTa Vec
WT LTa RasV12
Ts16 LTa RasV12

Figure S2, related to Figure 1. Transduction of trisomic MEFs with oncogenes.

(A) Western blot analysis of transgene expression levels in MEFs trisomic for mChr13, 16, or 19, transduced with p53dd or MYC. β-actin served as a loading control.

(B and C) Karyotypes of MEF lines that were transduced with (B) one oncogene or (C) two oncogenes were determined by low-pass whole genome sequencing. Note that the sequence results from the Ts1+p53dd+Ras^{V12} and control cell lines are reproduced in Figure 7.

Table S1, related to Figure 1. Oncogenes present on mouse chromosomes 1, 13, 16, and 19.†

Chr.	Gene Symbol	Name
1	ELK4	ELK4, ETS-domain protein (SRF accessory protein 1)
1	FCGR2B	Fc fragment of IgG, low affinity IIb, receptor for (CD32)
1	H3F3A	H3 histone, family 3A
1	MDM4	Mdm4 p53 binding protein homolog
1	PBX1	pre-B-cell leukemia transcription factor 1
1	SLC45A3	solute carrier family 45, member 3
1	TPR	translocated promoter region
1	CREB1	cAMP responsive element binding protein 1
1	FEV	FEV protein - (HSRNAFEV)
1	IDH1	isocitrate dehydrogenase 1 (NADP+), soluble
1	PAX3	paired box gene 3
1	SF3B1	splicing factor 3b, subunit 1, 155kDa
1	NCOA2	nuclear receptor coactivator 2 (TIF2)
1	TCEA1	transcription elongation factor A (SII), 1
1	BCL2	B-cell CLL/lymphoma 2
1	ABL2	c-abl oncogene 2, non-receptor tyrosine kinase
1	PMX1	paired mesoderm homeo box 1
1	ACSL3	acyl-CoA synthetase long-chain family member 3
1	ATIC	5-aminoimidazole-4-carboxamide ribonucleotide formyltransferase/IMP cyclohydrolase
1	CMKOR1	chemokine orphan receptor 1
1	LAF4	lymphoid nuclear protein related to AF4
1	FVT1	follicular lymphoma variant translocation 1
1	KDSR	3-ketodihydrosphingosine reductase [Source:MGI Symbol;Acc:MGI:1918000]
1	LHX4	LIM homeobox protein 4 [Source:MGI Symbol;Acc:MGI:101776]
1	FCGR3	Fc receptor, IgG, low affinity III [Source:MGI Symbol;Acc:MGI:95500]
1	CSNK2A1	casein kinase 2, alpha 1 polypeptide [Source:MGI Symbol;Acc:MGI:88543]
13	FGFR4	fibroblast growth factor receptor 4
13	IL6ST	interleukin 6 signal transducer (gp130, oncostatin M receptor)
13	NSD1	nuclear receptor binding SET domain protein 1
13	TERT	telomerase reverse transcriptase
13	DEK	DEK oncogene (DNA binding)
13	IRF4	interferon regulatory factor 4
13	TRIM27	tripartite motif-containing 27
13	OMD	osteomodulin
13	HIST1H3B	histone cluster 1, H3b
13	HIST1H4I	histone 1, H4i (H4FM)
13	SYK	spleen tyrosine kinase
13	NUTM2A	NUT family member 2A
13	NUTM2B	NUT family member 2B
13	NET1	neuroepithelial cell transforming gene 1 [Source:MGI Symbol;Acc:MGI:1927138]

13	RASA1	RAS p21 protein activator 1 [Source:MGI Symbol;Acc:MGI:97860]
13	SPZ1	Spermatogenic leucine zipper protein 1 (BHLH-Zip transcription factor SPZ1) (Spermatogenic Zip 1)
16	BCL6	B-cell CLL/lymphoma 6
16	EIF4A2	eukaryotic translation initiation factor 4A, isoform 2
16	ETV5	ets variant gene 5
16	LPP	LIM domain containing preferred translocation partner in lipoma
16	TFG	TRK-fused gene
16	TFRC	transferrin receptor (p90, CD71)
16	CIITA	class II, major histocompatibility complex, transactivator
16	MYH11	myosin, heavy polypeptide 11, smooth muscle
16	TNFRSF17	tumor necrosis factor receptor superfamily, member 17
16	ERG	v-ets erythroblastosis virus E26 oncogene like (avian)
16	OLIG2	oligodendrocyte lineage transcription factor 2 (BHLHB1)
16	RUNX1	runt-related transcription factor 1 (AML1)
16	TMPRSS2	transmembrane protease, serine 2
16	C16orf75	chromosome 16 open reading frame 75
16	RUNDC2A	RUN domain containing 2A
16	BCL5	B-cell CLL/lymphoma 5
16	PNUTL1	peanut-like 1 (Drosophila)
16	IGL	immunoglobulin lambda locus
16	LITAF	LPS-induced TN factor [Source:MGI Symbol;Acc:MGI:1929512]
16	ETS2	E26 avian leukemia oncogene 2, 3' domain [Source:MGI Symbol;Acc:MGI:95456]
19	CD274	CD274 molecule
19	GNAQ	guanine nucleotide binding protein (G protein), q polypeptide
19	JAK2	Janus kinase 2
19	NFKB2	nuclear factor of kappa light polypeptide gene enhancer in B-cells 2 (p49/p100)
19	NT5C2	5'-nucleotidase, cytosolic II
19	TCF7L2	transcription factor 7-like 2
19	TLX1	T-cell leukemia, homeobox 1 (HOX11)
19	VTI1A	vesicle transport through interaction with t-SNAREs homolog 1A
19	MALAT1	metastasis associated lung adenocarcinoma transcript 1 (lnc-RNA; non-protein coding)
19	CD273	programmed cell death 1 ligand 2
19	KIAA1598	KIAA1598
19	MXI1	Max interacting protein 1 [Source:MGI Symbol;Acc:MGI:97245]

† Data are derived from the Sanger Cancer Genome Census and the Uniprot list of proto-oncogenes.

A

Ts13

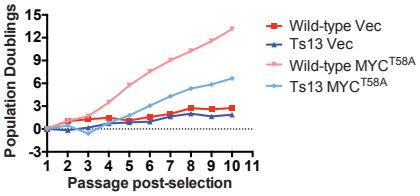

Ts16

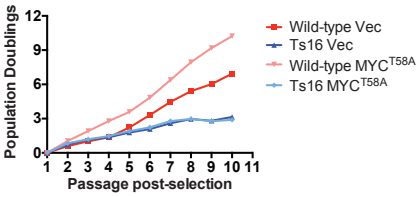

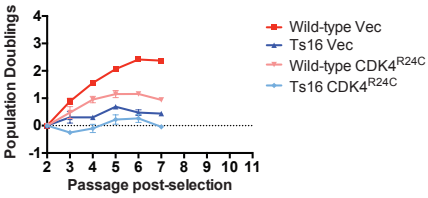

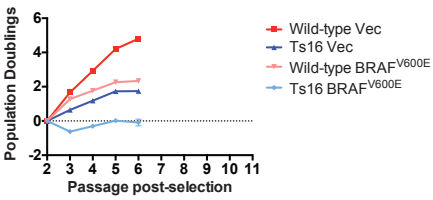

B

Ts13

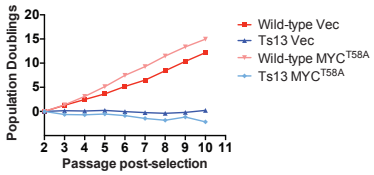

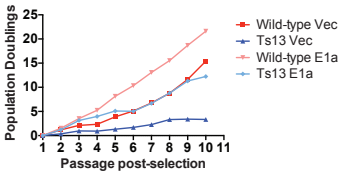

Ts16

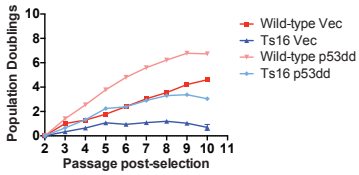

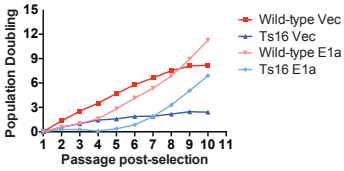

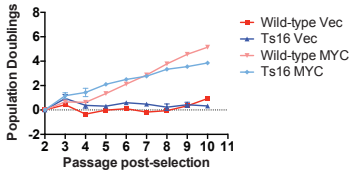

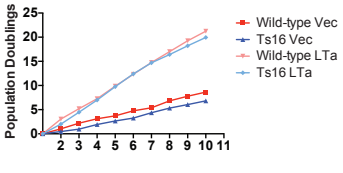

Ts19

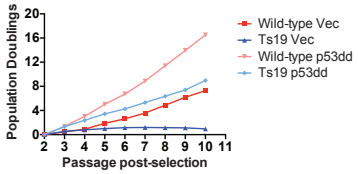

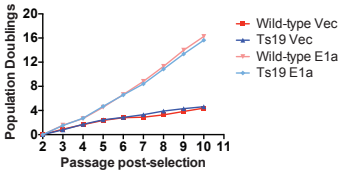

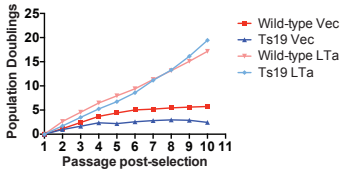

Figure S3, related to Figure 2. Additional single-oncogene experiments in trisomic and euploid fibroblasts.

(A) Euploid and trisomic cell lines were transduced with plasmids harboring the indicated oncogene or a matched empty vector. Following selection, the cell lines were passaged every third day for up to 10 passages, and the cumulative population doublings were determined. Experiments with $BRAF^{V600E}$ and $CDK4^{R24C}$ were terminated prematurely as both euploid and trisomic cells senesced following transduction.

(B) Nine single-oncogene transduction experiments were repeated in different, independently-derived cell lines. These lines were stably transduced with plasmids harboring the indicated oncogene(s) or a matched empty vector, and then passaged every third day for up to 10 passages. Some variability exists between replicates (e.g., compare Ts16+MYC in Figure S3B and Figure 2A), but no trisomy+oncogene combination was found to consistently outgrow a matched euploid line across multiple cell lines. Note that the panel displaying Ts19+LTa is reproduced in Figure S7.

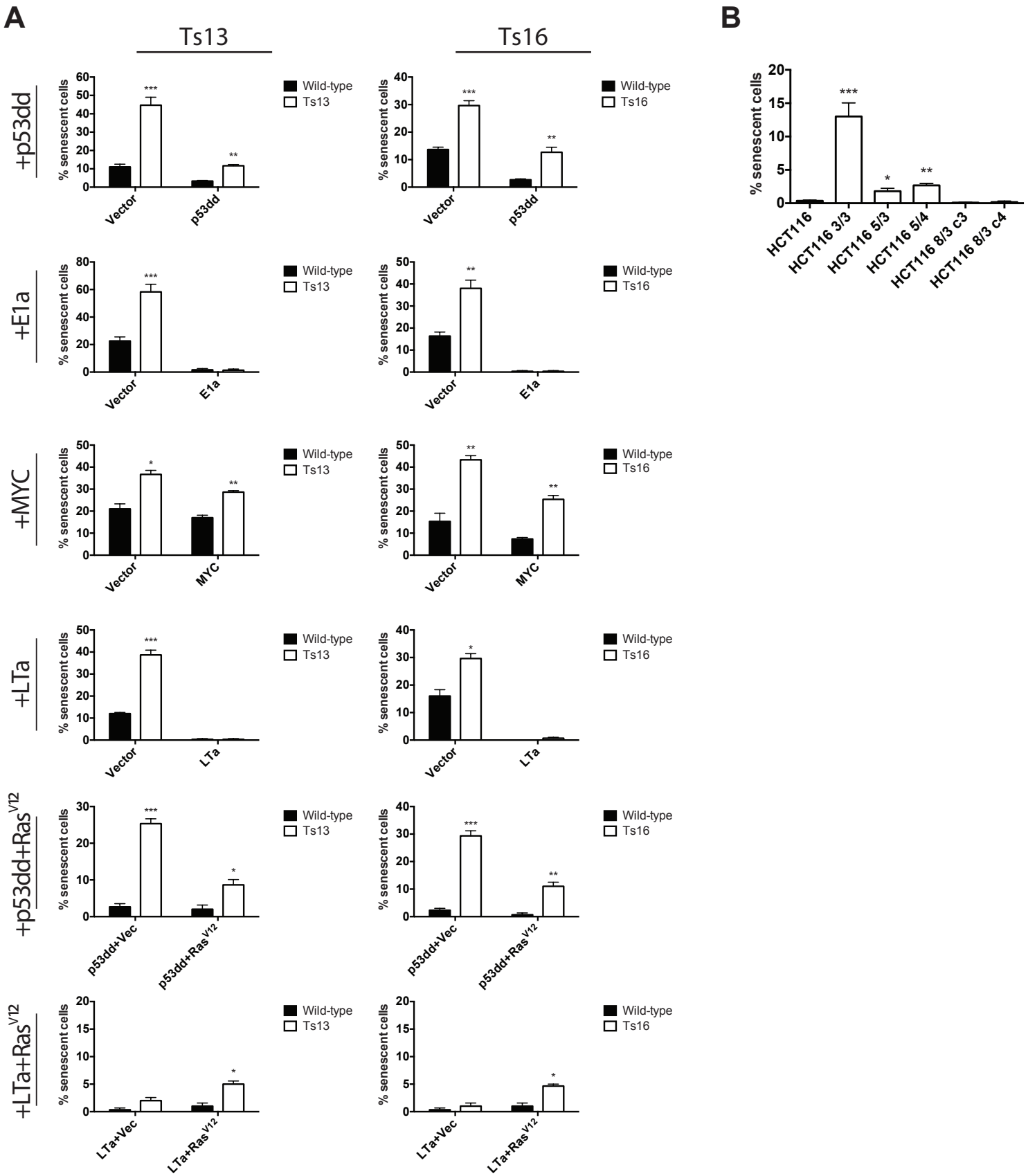
A
Ts13
Ts16
+p53dd
+E1a
+MYC
+LTa
+p53dd+Ras V12
+LTa+Ras V12
% senescent cells
Wild-type
Ts13
Ts16
Vector
p53dd
E1a
MYC
LTa
p53dd+Vec
p53dd+Ras V12
LTa+Vec
LTa+Ras V12
B
HCT116
HCT116 3/3
HCT116 5/3
HCT116 5/4
HCT116 8/3 c3
HCT116 8/3 c4

Figure S4, related to Figure 2. Trisomic cells display elevated levels of senescence-associated β-galactosidase.

At passage 6-8 in culture, the indicated cells were plated and stained for the expression of β-galactosidase. At least 200 cells in three wells were counted for each experiment. *, $p<.05$; **, $p<.005$; ***, $p<.0005$ (Student's t test). Error bars indicate the standard error of the mean.

A

Ts13

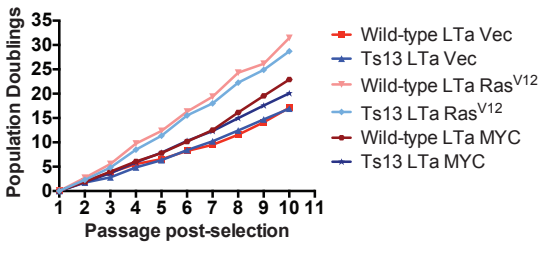

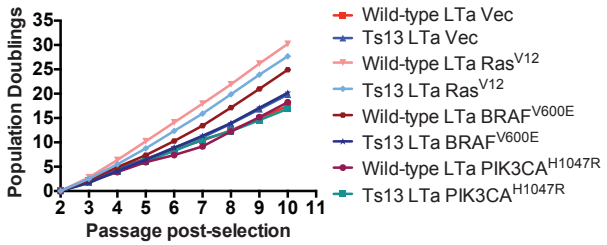

Ts16

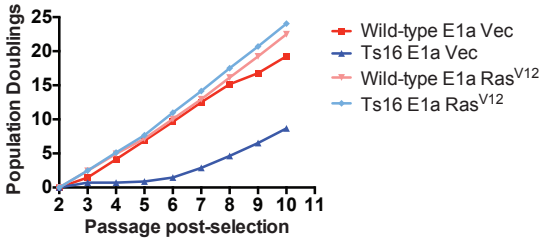

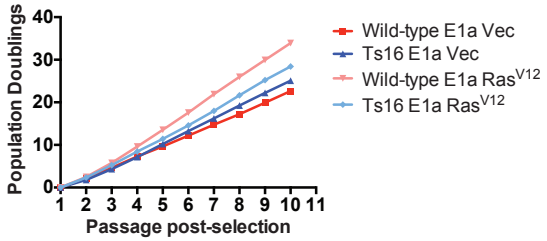

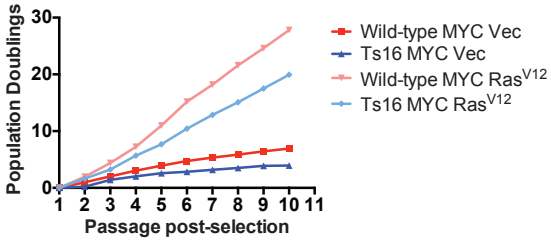

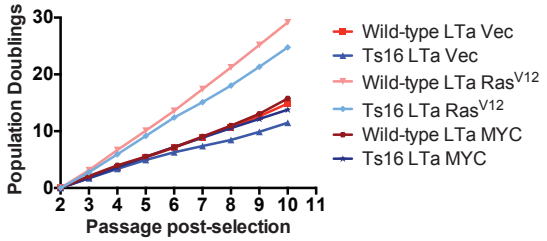

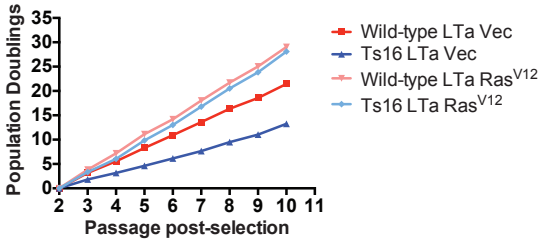

Ts19

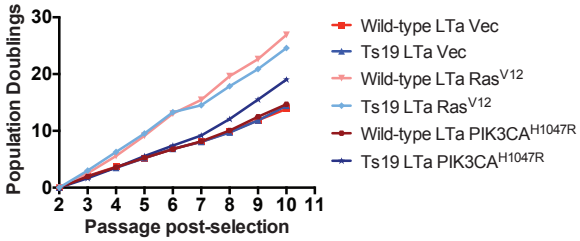

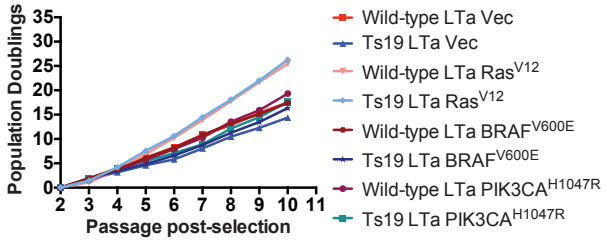

B

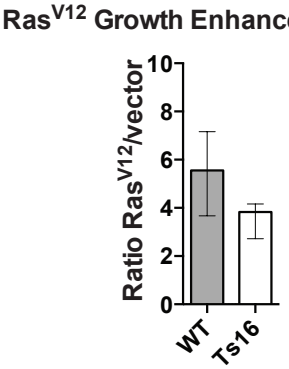

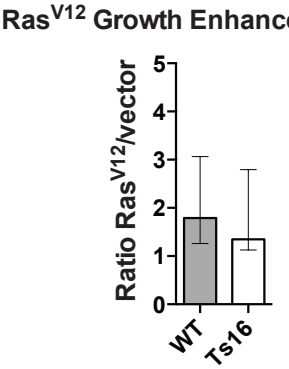

Figure S5, related to Figure 3. Additional double-oncogene cocktails and replicate experiments in trisomic MEFs.

(A) Euploid and trisomic cell lines were stably transduced with plasmids harboring the indicated oncogene or a matched empty vector. Following selection, the cell lines were passaged every third day for up to 10 passages, and the cumulative population doublings over the course of each experiment are displayed. Note that one replicate of Ts13+LTA+Vec and +Ras^{V12} and one replicate of Ts19+LTa+Vec and +Ras^{V12} are also presented in Figure 3A; these growth assays were conducted in parallel with growth assays in cells that harbor $BRAF^{V600E}$ or $PIK3CA^{H1047R}$ and are therefore shown here for comparison. Both Ts19+LTa experiments are also reproduced in Figure S7.

(B) The number of cells recovered from MYC+Ras^{V12}-transduced and E1a+ Ras^{V12}-transduced MEFs was divided by the number of cells recovered from vector-transduced MEFs at every passage. Bar graphs display the median ratios and the interquartile ranges. * p<.05; *** p<.0005 (Wilcoxon rank-sum test).

A

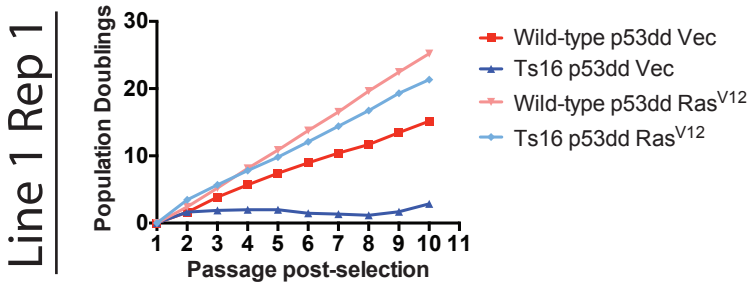
Line 1 Rep 1
Population Doublings
Passage post-selection
Wild-type p53dd Vec
Ts16 p53dd Vec
Wild-type p53dd Ras^{V12}
Ts16 p53dd Ras^{V12}

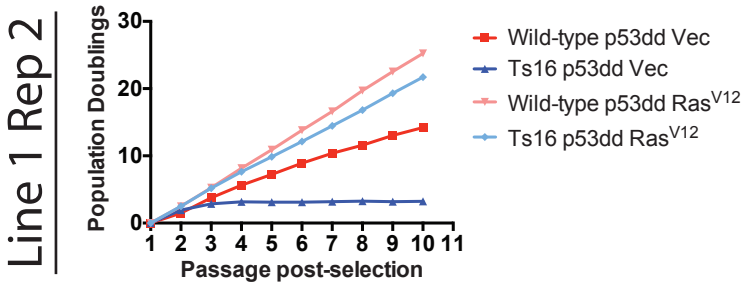
Line 1 Rep 2
Population Doublings
Passage post-selection
Wild-type p53dd Vec
Ts16 p53dd Vec
Wild-type p53dd Ras^{V12}
Ts16 p53dd Ras^{V12}

B

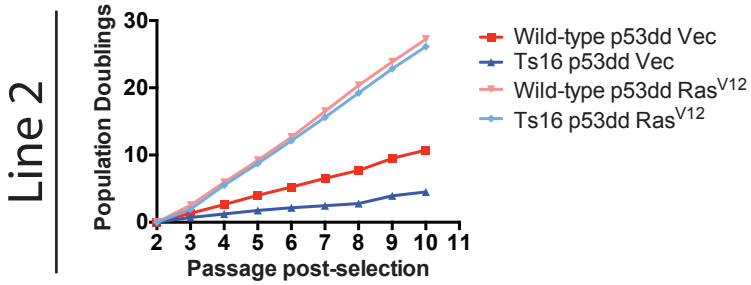
Line 2
Population Doublings
Passage post-selection
Wild-type p53dd Vec
Ts16 p53dd Vec
Wild-type p53dd Ras^{V12}
Ts16 p53dd Ras^{V12}

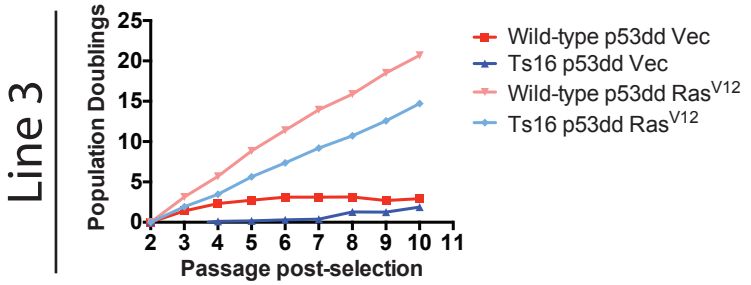
Line 3
Population Doublings
Passage post-selection
Wild-type p53dd Vec
Ts16 p53dd Vec
Wild-type p53dd Ras^{V12}
Ts16 p53dd Ras^{V12}

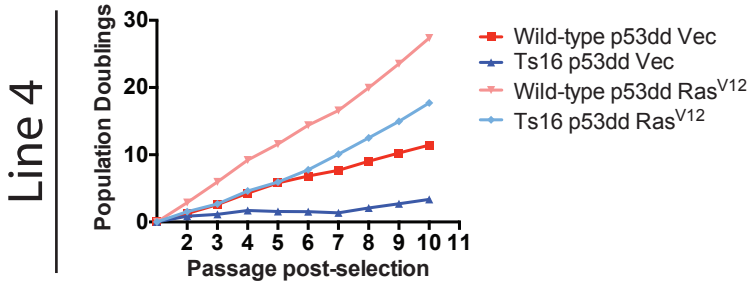
Line 4
Population Doublings
Passage post-selection
Wild-type p53dd Vec
Ts16 p53dd Vec
Wild-type p53dd Ras^{V12}
Ts16 p53dd Ras^{V12}

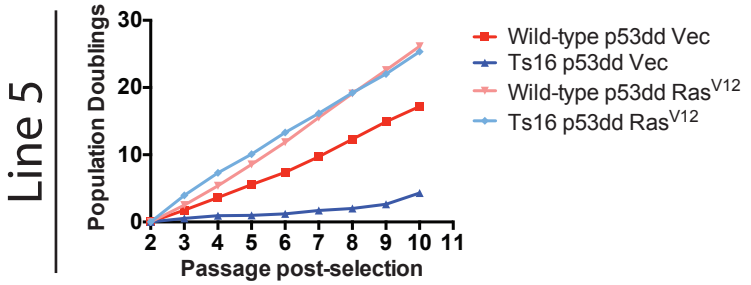
Line 5
Population Doublings
Passage post-selection
Wild-type p53dd Vec
Ts16 p53dd Vec
Wild-type p53dd Ras^{V12}
Ts16 p53dd Ras^{V12}

Figure S6, related to Figure 3. Replicate growth curves of the same or of independently-derived Ts16 cells that express p53dd and Ras^{V12}.

(A) The same WT and Ts16 MEF lines were stably transduced with plasmids harboring the indicated oncogene or a matched empty vector. Following selection, the cell lines were passaged every third day for up to 10 passages, and the cumulative population doublings over the course of each experiment are displayed. Note that Line 1 Rep 1 is also displayed in Figure 2A.

(B) Four independently derived pairs of WT or Ts16 MEFs were transduced and passaged as described above. Error bars indicate the standard error of the mean.

Table S2, related to Figure 5. Oncogenes present on human chromosomes 3, 5, and 8.†

Chr.	Gene Symbol	Name
3	BCL6	B-cell CLL/lymphoma 6
3	CTNNB1	catenin (cadherin-associated protein), beta 1
3	CCNL1	Cyclin-L1 (Cyclin-L)
3	DCUN1D1	DCN1-like protein 1 (DCUN1 domain-containing protein 1) (Defective in cullin neddylation protein 1-like protein 1) (Squamous cell carcinoma-related oncogene)
3	EVI1	ecotropic viral integration site 1
3	ETV5	ets variant gene 5
3	EIF4A2	eukaryotic translation initiation factor 4A, isoform 2
3	FOXL2	forkhead box L2
3	FOXP1	forkhead box P1
3	FHIT	fragile histidine triad gene
3	GATA2	GATA binding protein 2
3	GMPS	guanine monphosphate synthetase
3	LPP	LIM domain containing preferred translocation partner in lipoma
3	MECOM	MDS1 and EVI1 complex locus protein EVI1 (Ecotropic virus integration site 1 protein homolog) (EVI-1)
3	MITF	microphthalmia-associated transcription factor
3	MDS1	myelodysplasia syndrome 1
3	MYD88	myeloid differentiation primary response gene (88)
3	MLF1	myeloid leukemia factor 1
3	NCKIPSD	NCK-interacting protein with SH3 domain (54 kDa VacA-interacting protein) (54 kDa vimentin-interacting protein) (VIP54) (90 kDa SH3 protein interacting with Nck) (AF3p21) (Dia-interacting protein 1) (DIP-1) (Diaphanous protein-interacting protein) (SH3 adapter protein SPIN90) (WASP-interacting SH3-domain protein) (WISH) (Wiskott-Aldrich syndrome protein-interacting protein)
3	PPARG	peroxisome proliferative activated receptor, gamma
3	PIK3CA	phosphoinositide-3-kinase, catalytic, alpha polypeptide
3	PRKCI	Protein kinase C iota type (EC 2.7.11.13) (Atypical protein kinase C-lambda/iota) (PRKC-lambda/iota) (aPKC-lambda/iota) (nPKC-iota)
3	RHOA	ras homolog family member A
3	RARB	Retinoic acid receptor beta (RAR-beta) (HBV-activated protein) (Nuclear receptor subfamily 1 group B member 2) (RAR-epsilon)
3	RPN1	ribophorin I
3	AF3p21	SH3 protein interacting with Nck, 90 kDa (ALL1 fused gene from 3p21)
3	SRGAP3	SLIT-ROBO Rho GTPase activating protein 3
3	SOX2	SRY (sex determining region Y)-box 2
3	TCTA	T-cell leukemia translocation-altered gene protein (T-cell leukemia translocation-associated gene protein)

3	TFRC	transferrin receptor (p90, CD71)
3	TFG	TRK-fused gene
3	USP4	Ubiquitin carboxyl-terminal hydrolase 4 (EC 3.4.19.12) (Deubiquitinating enzyme 4) (Ubiquitin thioesterase 4) (Ubiquitin-specific-processing protease 4) (Ubiquitous nuclear protein homolog)
3	RAF1	v-raf-1 murine leukemia viral oncogene homolog 1
3	WWTR1	WW domain containing transcription regulator 1
3	ZNF9	zinc finger protein 9 (a cellular retroviral nucleic acid binding protein)
5	AFF4	AF4/FMR2 family member 4 (ALL1-fused gene from chromosome 5q31 protein) (Protein AF-5q31) (Major CDK9 elongation factor-associated protein)
5	AF5q31	ALL1 fused gene from 5q31
5	CD74	CD74 molecule, major histocompatibility complex, class II invariant chain
5	EBF1	early B-cell factor 1
5	FACL6	fatty-acid-coenzyme A ligase, long-chain 6
5	FGFR4	fibroblast growth factor receptor 4
5	GRAF	GTPase regulator associated with focal adhesion kinase pp125(FAK)
5	ITK	IL2-inducible T-cell kinase
5	IL6ST	interleukin 6 signal transducer (gp130, oncostatin M receptor)
5	IL7R	interleukin 7 receptor
5	LIFR	leukemia inhibitory factor receptor
5	CSF1R	Macrophage colony-stimulating factor 1 receptor (CSF-1 receptor) (CSF-1-R) (CSF-1R) (M-CSF-R) (EC 2.7.10.1) (Proto-oncogene c-Fms) (CD antigen CD115)
5	NSD1	nuclear receptor binding SET domain protein 1
5	NPM1	nucleophosmin (nucleolar phosphoprotein B23, numatrin)
5	PDGFRB	platelet-derived growth factor receptor, beta polypeptide
5	PWWP2A	PWWP domain containing 2A
5	RANBP17	RAN binding protein 17
5	RASA1	Ras GTPase-activating protein 1 (GAP) (GTPase-activating protein) (RasGAP) (Ras p21 protein activator) (p120GAP)
5	ARHGAP26	Rho GTPase-activating protein 26 (GTPase regulator associated with focal adhesion kinase) (Oligophrenin-1-like protein) (Rho-type GTPase-activating protein 26)
5	PTTG1	Securin (Esp1-associated protein) (Pituitary tumor-transforming gene 1 protein) (Tumor-transforming protein 1) (hPTTG)
5	TLX3	T-cell leukemia, homeobox 3 (HOX11L2)
5	TERT	telomerase reverse transcriptase
5	FER	Tyrosine-protein kinase Fer (EC 2.7.10.2) (Feline encephalitis virus-related kinase FER) (Fujinami poultry sarcoma/Feline sarcoma-related protein Fer) (Proto-oncogene c-Fer) (Tyrosine kinase 3) (p94-Fer)
8	CHCHD7	coiled-coil-helix-coiled-coil-helix domain containing 7
8	CBFA2T1	core-binding factor, runt domain, alpha subunit 2;translocated to, 1 (ETO)

8	COX6C	cytochrome c oxidase subunit VIc
8	EIF3E	eukaryotic translation initiation factor 3, subunit E
8	FGFR1	fibroblast growth factor receptor 1
8	HEY1	hairy/enhancer-of-split related with YRPW motif 1
8	KAT6A	Histone acetyltransferase KAT6A (EC 2.3.1.48) (MOZ, YBF2/SAS3, SAS2 and TIP60 protein 3) (MYST-3) (Monocytic leukemia zinc finger protein) (Runt-related transcription factor-binding protein 2) (Zinc finger protein 220)
8	HOOK3	hook homolog 3
8	IKBKB	inhibitor of kappa light polypeptide gene enhancer in B-cells, kinase beta
8	NRG1	neuregulin 1
8	NDRG1	N-myc downstream regulated 1
8	NCOA2	nuclear receptor coactivator 2 (TIF2)
8	PCM1	pericentriolar material 1 (PTC4)
8	PLAG1	pleiomorphic adenoma gene 1
8	RUNX1T1	Protein CBFA2T1 (Cyclin-D-related protein) (Eight twenty one protein) (Protein ETO) (Protein MTG8) (Zinc finger MYND domain-containing protein 2)
8	MOS	Proto-oncogene serine/threonine-protein kinase mos (EC 2.7.11.1) (Oocyte maturation factor mos) (Proto-oncogene c-Mos)
8	RSPO2	R-spondin 2
8	RUNXBP2	runt-related transcription factor binding protein 2 (MOZ/ZNF220)
8	TCEA1	transcription elongation factor A (SII), 1
8	MAFA	Transcription factor MafA (Pancreatic beta-cell-specific transcriptional activator) (Transcription factor RIPE3b1) (V-maf musculoaponeurotic fibrosarcoma oncogene homolog A)
8	LYN	Tyrosine-protein kinase Lyn (EC 2.7.10.2) (Lck/Yes-related novel protein tyrosine kinase) (V-yes-1 Yamaguchi sarcoma viral related oncogene homolog) (p53Lyn) (p56Lyn)
8	MYC	v-myc myelocytomatosis viral oncogene homolog (avian)
8	WISP1	WNT1-inducible-signaling pathway protein 1 (WISP-1) (CCN family member 4) (Wnt-1-induced secreted protein)
8	WHSC1L1	Wolf-Hirschhorn syndrome candidate 1-like 1 (NSD3)

† Data are derived from the Sanger Cancer Genome Census and the Uniprot list of proto-oncogenes.

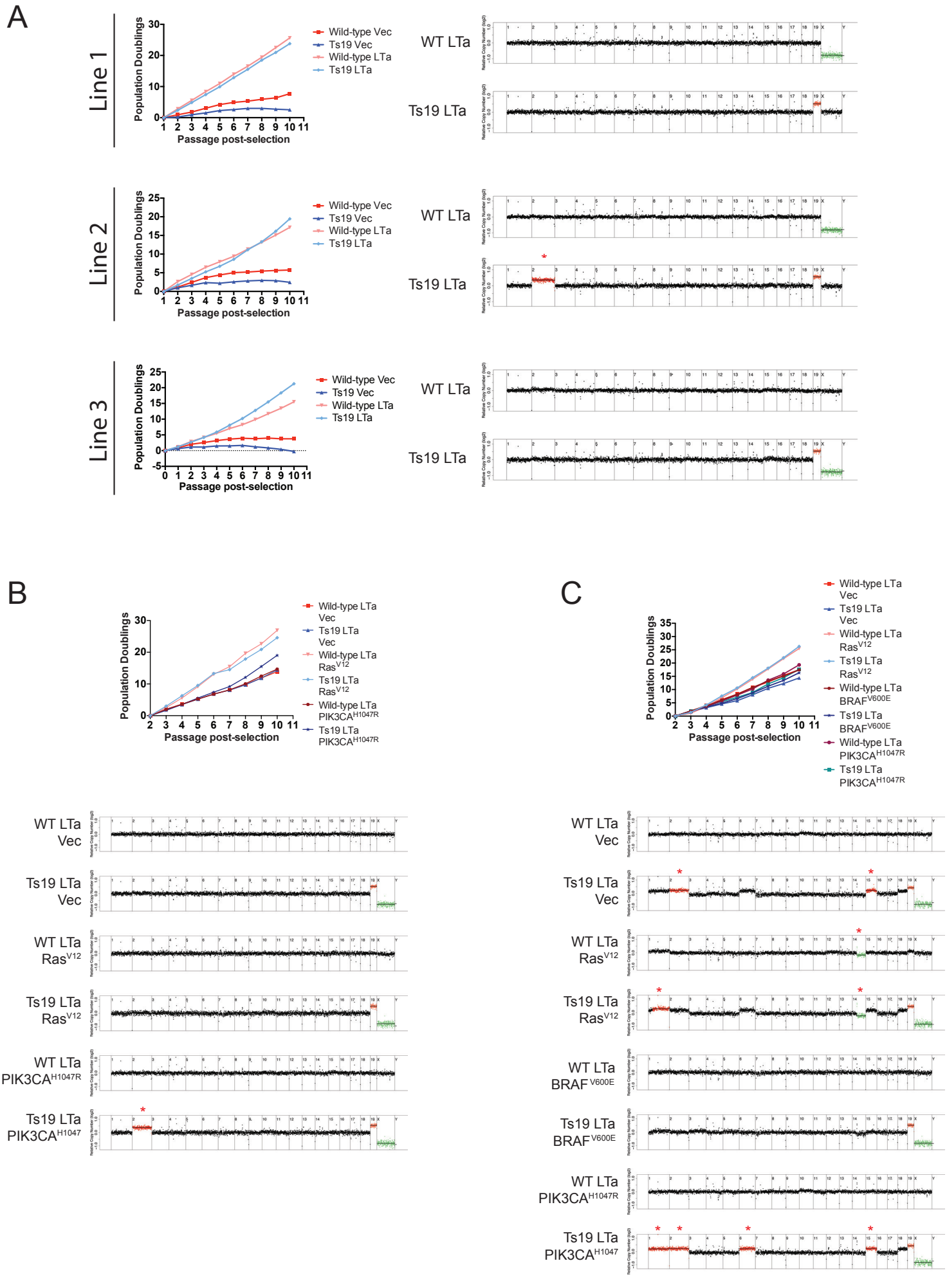
A
Line 1
Line 2
Line 3
Population Doublings
Passage post-selection
Wild-type Vec
Ts19 Vec
Wild-type LTa
Ts19 LTa
WT LTa
Ts19 LTa
B
C
Wild-type LTa Vec
Ts19 LTa Vec
Wild-type LTa RasV12
Ts19 LTa RasV12
Wild-type LTa PIK3CAH1047R
Ts19 LTa PIK3CAH1047R
Wild-type LTa BRAFV600E
Ts19 LTa BRAFV600E
WT LTa Vec
Ts19 LTa Vec
WT LTa RasV12
Ts19 LTa RasV12
WT LTa PIK3CAH1047R
Ts19 LTa PIK3CAH1047
WT LTa BRAF V600E
Ts19 LTa BRAFV600E

Figure S7, related to Figure 7. Analysis of Ts19 MEF lines transduced with LTa.

(A) Ts19 MEF lines and matched euploid control cell lines were transduced with LTa or with an empty vector and then passaged every third day for up to 10 passages. Lines 2 and 3 exhibited a growth inflection after several passages and overtook the wild-type cells. Sequence analysis at late passage revealed an extra copy of chromosome 2 (indicated with an asterisk) in the second Ts19 line. Note that line 1 is also displayed in Figure 2A, and line 2 is also displayed in Figure S3. Deviations from each cell line's initial karyotype are indicated with an asterisk.

(B) Ts19 cell line and a matched euploid control cell line were transduced with Large T, and then transduced a second time with an empty vector, Ras^{V12}, or $PIK3CA^{H1047R}$. The Ts19+LTa+$PIK3CA^{H1047R}$ cell line grew more rapidly than an equivalently-transduced euploid line. Sequencing at passage 10 revealed that the Ts19+LTa+$PIK3CA^{H1047R}$ line had acquired an extra copy of chromosome 2, while the other cell lines showed no other deviations from the expected karyotypes.

(C) A second Ts19 cell line and a matched euploid control cell line were transduced with LTa, and then transduced a second time with an empty vector, Ras^{V12}, $BRAF^{V600E}$, or $PIK3CA^{H1047R}$. All euploid/Ts19 pairs grew at approximately the same rates over the course of the experiment. Read depth analysis at passage 10 revealed several karyotypic alterations, including a gain of mChr2. Note that the growth curves displayed in A and B are also presented in Figure 3A and Figure S5. Deviations from each cell line's initial karyotype are indicated with an asterisk.

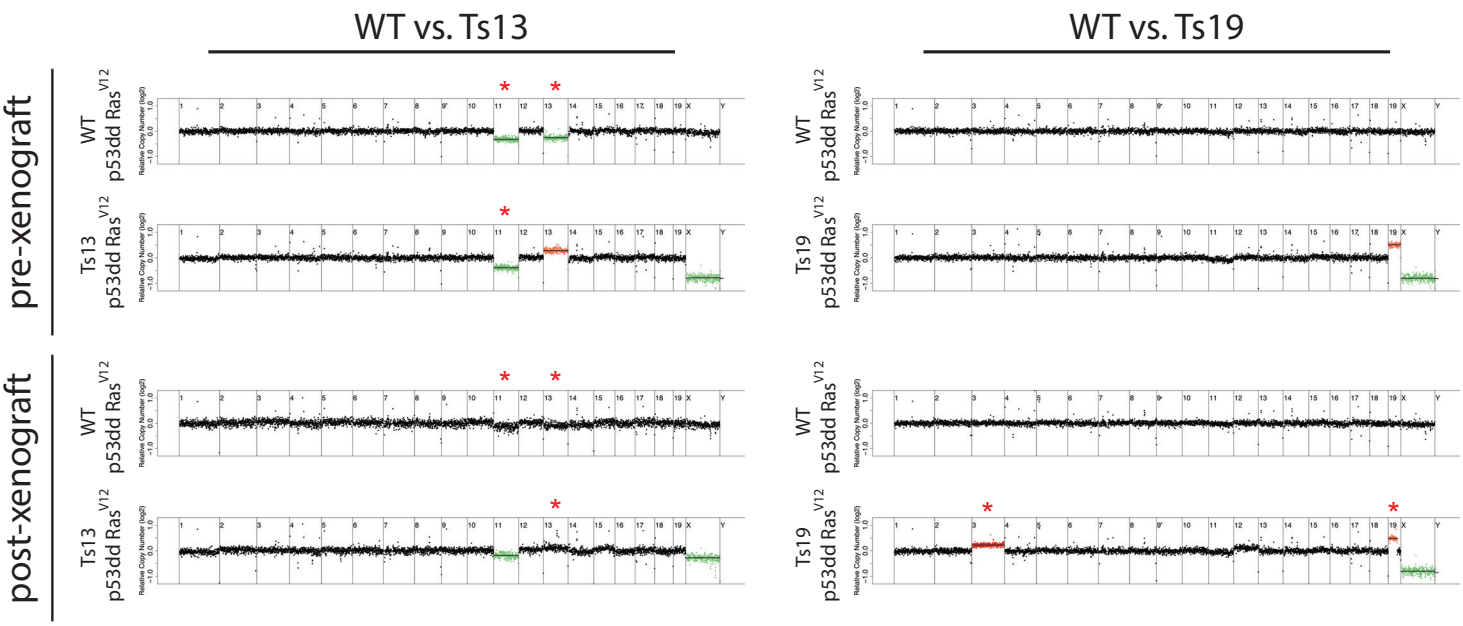
WT vs. Ts13
WT vs. Ts19
pre-xenograft
post-xenograft
WT p53dd Ras V12
Ts13 p53dd Ras V12
Ts19 p53dd Ras V12

Figure S8, related to Figure 7. Karyotype evolution of transformed MEFs during xenograft growth.

Cell lines trisomic for mChr13 or mChr19, as well as matched euploid control cells, were transduced with p53dd and Ras^{V12}, expanded for several passages to increase cell number, and then injected subcutaneously into nude mice. DNA from each cell line before and after xenograft growth was subjected to low-pass whole genome sequencing, and the derived karyotypes of each cell line are displayed. Deviations from each cell line's initial karyotype are indicated with an asterisk.

Supplemental Experimental Procedures

MEF derivation, culture, and transduction

A Robertsonian breeding scheme was utilized to generate sibling-matched euploid and trisomic MEFs as described in Williams et al., 2008. Note that due to the extreme fitness defect caused by the gain of chromosome 1, to date we have only been able to generate a MEF line from a single Ts1 embryo. Therefore, only single replicates of experiments involving this trisomy are displayed.

MEFs were cultured in DMEM supplemented with 10% FBS, 2mM glutamine, and 100 U/ml penicillin and streptomycin. Cells were maintained at 37° C and 5% CO_2 in a humidified environment. Cell counting was performed using the Cellometer Auto T4 system. Plasmids encoding oncogenes were obtained from Addgene (https://www.addgene.org/) and then transfected into the Phoenix-Eco cell line (Swift et al., 2001) using TransIT-LT1 (Mirus). Viral supernatants were collected 24, 48, and 72 hours post-transfection, and were applied to freshly-split passage 2 MEFs. Transduced cells were selected by FACS, or by the addition of puromycin (1.6 µg/ml), hygromycin (200 µg/ml), or G418 (1 mg/ml).

Human colon cancer cell culture

Aneuploid cell lines derived from HCT116 cells were previously described in Stingele et al., 2012 and Donnelly et al., 2014. Cells were cultured in DMEM supplemented with 10% FBS, 2mM glutamine, and 100 U/ml penicillin and streptomycin. Cells were maintained at 37° C and 5% CO_2 in a humidified environment.

Low-pass whole genome sequencing

Sequencing reactions were performed at the MIT BioMicro Center. 50 ng of purified DNA from each cell line were prepared and barcoded using Nextera reagents (Illumina), and tagmented material was PCR amplified for seven cycles. Libraries were quantified using an

AATI Fragment Analyzer before pooling. Libraries were sequenced (40bp read length) on an Illumina HiSeq2000. Reads were demultiplexed using custom scripts allowing single mismatches within the reference barcode.

Sequence reads were trimmed to 40 nucleotides and aligned to the mouse (mm9) or human (hg19) genomes using BWA (0.6.1) with default options (Li and Durbin, 2009). HMMcopy (0.1.1) was used to detect copy number alterations by estimating copy number in 500-kb bins controlling for mappability [downloaded from UCSC Genome Bioinformatics (http://hgdownload.cse.ucsc.edu/goldenPath/hg19/encodeDCC/wgEncodeMapability/ or http://hgdownload.cse.ucsc.edu/goldenPath/mm9/encodeDCC/wgEncodeMapability/)] and GC content (calculated by HMMcopy gcCounter)(Ha et al., 2012).

Cell proliferation and tumorigenicity assays

For proliferation assays, MEFs and HCT116 cells were passaged using a modified 3T3 protocol (Todaro and Green, 1963). $3x10^5$ cells were plated in three wells of a 6-well plate, and cells were combined, counted, and re-plated at the same density every third day. For focus formation assays, 1000 cells (MEFs) or 200 cells (HCT116) were plated in triplicate on 10cm plates, and then allowed to grow for 10 (MEFs) or 14 days (HCT116). Subsequently, colonies were fixed with ice-cold 100% methanol for 10 minutes, and then stained with a solution of 0.5% crystal violet in 25% methanol for 10 minutes. For soft agar assays, a 1% base layer of Difco Agar Noble was prepared and then mixed with an equal amount of 2X DMEM. The solution (0.5% agar in 1X DMEM) was then added to each well of a 6-well plate and allowed to solidify. Subsequently, a top layer of 0.7% agar was prepared and mixed with an equal volume of a 2X solution of DMEM containing 10,000 cells (MEFs) or 2000 cells (HCT116) and added to the base layer in triplicate. The plates were incubated for 20 days at 37° C prior to imaging.

For xenograft studies, 5 - 10 female, 5-week old Nu/J mice (Jackson Laboratory Stock 002019) were utilized for each experiment. Cells to be injected were harvested and

concentrated to 10^7 (MEFs) or $4x10^7$ (HCT116) cells/ml in PBS. 100µl of the solution was injected subcutaneously into the rear flanks of each mouse using a 25 gauge needle. Euploid and aneuploid cell lines were typically injected contralaterally, with the exception of experiments involving cell lines transduced with LTa and Ras^{V12}, in which only one cell line was injected into each animal. Tumor dimensions were measured every third day using calipers, and tumor volumes were calculated using the formula $0.5 \times A \times B^2$, where A is the longer diameter and B is the shorter diameter. H&E staining of paraformaldehyde-fixed sections was performed according to standard methods. All animal studies and procedures were approved by the MIT Institutional Animal Care and Use Committee.

Immunoblotting

Cells were lysed with RIPA buffer (50 mM Tris-HCl at pH7.4, 150 mM NaCl, 5 mM $MgCl_2$, 1% Triton X-100, 0.5% NP-40, 10% glycerol, protease inhibitor cocktail [Roche], phosphatase inhibitor cocktail [Roche]). The lysate was run on a 12% (Myc) or 14% (p53dd) SDS-PAGE gel and transferred to a nitrocellulose membrane. The membrane was then probed with the following primary antibodies: anti-c-Myc (Abcam, ab32072), anti-p53 (Santa Cruz Biotechnology, sc-6243), or anti-β-actin (Sigma-Aldrich, A2228). The following secondary antibodies were used: HRP anti-rabbit (GE Healthcare, NA934V) or HRP anti-mouse (GE Healthcare, NA9310V). The protein was then detected using enhanced chemiluminescence (GE Healthcare, RPN2232).

β-galactosidase staining

5000 cells of each cell line were plated in triplicate in a 48-well plate, allowed to attach overnight, and then stained using a Senescence Histochemical Staining Kit (Sigma-Aldritch). Cells were incubated in the X-gal solution overnight at 37° C prior to imaging on a Nikon Eclipse TE2000.

Competition experiments

To directly compare the fitness of the aneuploid and near-euploid HCT116 cell lines, we mixed equal numbers of GFP+ aneuploid HCT116 with a GFP+ DsRed+ near-euploid HCT116 line. Every third day, the cells were trypsinized, replated, and an aliquot was removed for analysis on a MacsQuant Analyzer 10 (Milltenyi Biotec).

Supplemental References

Ha, G., Roth, A., Lai, D., Bashashati, A., Ding, J., Goya, R., Giuliany, R., Rosner, J., Oloumi, A., Shumansky, K., et al. (2012). Integrative analysis of genome-wide loss of heterozygosity and monoallelic expression at nucleotide resolution reveals disrupted pathways in triple-negative breast cancer. Genome Res. *22*, 1995–2007.

Li, H., and Durbin, R. (2009). Fast and accurate short read alignment with Burrows–Wheeler transform. Bioinformatics *25*, 1754–1760.

Swift, S., Lorens, J., Achacoso, P., and Nolan, G.P. (2001). Rapid production of retroviruses for efficient gene delivery to mammalian cells using 293T cell-based systems. Curr. Protoc. Immunol. Ed. John E Coligan Al *Chapter 10*, Unit 10.17C.

Todaro, G.J., and Green, H. (1963). Quantitative Studies of the Growth of Mouse Embryo Cells in Culture and Their Development into Established Lines. J. Cell Biol. *17*, 299–313.